scientific reports

Check for updates

OPEN

Bioconvective flow of Maxwell nanoparticles with variable thermal conductivity and convective boundary conditions

Hassan Hanafy[1,2] & Iskander Tlili[1]✉

Owing to recent development in the thermal sciences, scientists are focusing towards the wide applications of nanofluids in industrial systems, engineering processes, medical sciences, enhancing the transport sources, energy production etc. In various available studies on nanomaterials, the thermal significance of nanoparticles has been presented in view of constant thermal conductivity and fluid viscosity. However, exponents verify that in many industrial and engineering process, the fluid viscosity and thermal conductivity cannot be treated as a constant. The motivation of current research is to investigates the improved thermal aspects of magnetized Maxwell nanofluid attaining the variable viscosity and thermal conductivity. The nanofluid referred to the suspension of microorganisms to ensure the stability. The insight of heat transfer is predicted under the assumptions of radiated phenomenon. Additionally, the variable thermal conductivity assumptions are encountered to examine the transport phenomenon. Whole investigation is supported with key contribution of convective-Nield boundary conditions. In order to evaluating the numerical computations of problem, a famous shooting technique is utilized. After ensuring the validity of solution, physical assessment of problem is focused. It is claimed that velocity profile boosted due to variable viscosity parameter. A reduction in temperature profile is noted due to thermal relaxation constant.

List of symbols

u, v	Velocity components
T	Temperature
T_∞	Ambient temperature
C	Concentration
ρ_f	Fluid density
B_0	Magnetic field strength
$\widetilde{K}(T)$	Variable thermal conductivity
D_B	Brownian diffusion
k^*	Mean absorption coefficient
Q_0	Heat source coefficient
Pr	The Prandtl number
R_d	The radiation parameter
β	The Maxwell parameter
ε	The Curie temperature parameter
N_t	The thermophoresis parameter
Pe	Peclet number
Nu_x	Local Nusselt number
Sh_x	Local Sherwood number
T_w	Surface temperature
C_∞	Ambient concentration

[1]Department of Physics, College of Science, Al-Zulfi, Majmaah University, 11952 Al-Majmaah, Saudi Arabia. [2]Physics Department, Faculty of Sciences, Beni-Suef University, Beni Suef 62514, Egypt. ✉email: I.tlili@mu.edu.sa

λ	Relaxation time
$\tilde{\tilde{\mu}}(T)$	Temperature dependent viscosity
σ	Electrical conductivity
ρc_p	Specific heat
q_r	Radiative flux
$\hat{b}$	Chemotaxis constant
Re_x	Local Reynolds number
D_m	Microorganisms diffusion constant
γ_1	The Biot number
Le	The Lewis number
M	Hartmann parameter
N_b	The Brownian motion parameter
Q	The heat source /sink parameter
δ_1	Microorganism difference parameter
C_{fx}	Skin friction coefficient
Nn_x	Motile density number

In recent developments in nanoscience's, the attention of researchers increases in study of nanofluids to suggests more valuables applications. Basically, nanofluids reports the decomposition of tiny metal particles with base materials. The fundamental aspects of nanomaterials are higher thermal capacitance and stable heating aspect. Diverse applications in modern engineering and technological systems is discussed for nanofluids in extrusion systems, engine of vehicles, nuclear reactions, cooling systems etc. In the modern medical sciences, scientists have contributed the applications of tiny particles in the cancer treatment and chemo-therapy. Choi[1] initiated the basic research on nanoparticles with support of novel experimental results. Kumar et al.[2] deduced the nanofluid role in enhancing heat transfer for non-Newtonian slip flow. Santos et al.[3] preserved the statistical analysis regarding nanofluid problem and suggested improved thermal performances. Sohail et al.[4] tested the Sutterby nanofluid conveying stretching cylinder via modified laws. Muhammad et al.[5] reported the hybrid class of nanofluid to boosted the quantitative impact of base liquid. Babazadeh et al.[6] discussed the shape factors for enclosure filled with nanoparticles in porous space. The lubricated constraints for nanofluid under the melting heating source was focused by Alqarni et al.[7]. Saeed et al.[8] examined the Darcy Forchheimer analysis for nanofluid in porous moving frame. Hamrelaine analyzed the convergent/divergent channel flow analysis subject to nanofluid. The esterification of nanofluid based on pressure driven phenomenon in circular surface have been evaluated by Shahzad et al.[10]. Acharya[11] observed the entropy generation aspects of copper nanofluid for natural convective flow. Sajid et al.[12] discussed the Reiner-Philippoff hybrid nanofluid with quadratic chemical analysis. The aluminum nanoparticles thermal attention was tested by Hanif et al.[13]. Iqbal et al.[14] justified the role of Lorentz force while incorporating nanofluid thermal prediction with slip features. Mabood et al.[15] organized the Wu's slip impact for nanofluid containing the variable thermal conductivity. Chu et al.[16] addressed the chemical reactive analysis for nanofluid via computational model.

The microorganisms floating due to lower densities causes the phenomenon of bioconvection. The suspension of microorganisms in upper regime is associated to the instability of uniform structure. The uniform movement of nanoparticles does not effect the suspension of microorganisms and signifies applications in biotechnology and bio-engineering. Alwatban et al.[17] addressed the bioconvection outcomes in Eyring-Powell nanofluid. Khan et al.[18] deduces bioconvective observations while defining the heating onset of thixotropic nanofluid. Khan et al.[19] analyzed the entropy generation framework in suspension of microorganisms in nanofluid. Bafakeeh et al.[20] examined the bioconvective onset in viscoelastic nanofluid. The features of activation energy in bioconvective flow was reported by Khan et al.[21]. Bhatti et al.[22] announced the higher order slip mechanism in nanofluid flow with microorganisms. Irfan[23] investigated the Joule heating impact for Maxwell nanofluid. Ali et al.[24] analyzed the joint rheology of Casson-Williamson nanofluid with significance of thermos-diffusion phenomenon. The nonlinear mixed convection flow associated to Carreau nanofluid was contributed by Irfan[25].

Continuous research in non-Newtonian materials is focused by investigators in recent years due to their prestigious applications in industrial systems and manufacturing processes. The novelty of non-Newtonian materials is dynamic and relatively complex. In order to evaluate the rheological aspects of nonlinear materials, difference non-Newtonian models are prosed in literature. In such categories, Maxwell fluid is one which occupies the interesting relaxation time features. Maxwell fluid model is important in manufacturing processes and cosmetics. Many studies are available which reports the rheology of Maxwell fluid. Some research on Maxwell nanofluid is seen in Refs.[27–29].

The aim of current research is to present the bioconvective flow of Maxwell nanofluid with in presence of thermal radiation and external heat source. The inspection of transport phenomenon is predicted under the assumptions of variable viscosity and variable thermal conductivity. Furthermore, analysis is subject to the activation energy. The convective-Nield thermal conditions are imposed to analyze the flow. The convective-Nield thermal constraints are associated to the consideration of convective conditions for heat and mass transfer phenomenon. The computations of problem are performed via shooting technique. Current investigation presents the answer to following research questions:

- How velocity profile of Maxwell nanofluid truncated for variable viscosity?
- What is the significance of temperature dependent thermal conductivity for enhancing the heat transfer rate?
- Why external heat source and radiative phenomenon is important to inspect the heat transfer rate?

- What is the contribution of bioconvection phenomenon in nanofluid flow?
- How does heat and mass transfer pattern fluctuated with interaction of convective-Nield thermal constraints?

Physical description and formulation of problem

Let us assumed a two-dimensional and steady transport of Maxwell nanofluid with suspension of microorganisms over stretched surface. The normal direction magnetic force is implemented. The variable consideration of viscosity is taken into contributed. The Cartesian system is used for modeling and configuration. The velocity components u and v are taken in horizontal and normal directions, respectively. Flow configuration is presented in Fig. 1. In concentration equation, the activation energy outcomes are utilized. The modification in energy equation is supported with radiative phenomenon and external heat source. Defining temperature, surface temperature, free stream temperature, concentration, and ambient concentration is defined as T, T_w, T_∞, C and C_∞, respectively. Moreover, n, n_w and n_∞ be motile density, surface motile density and free stream motile density, respectively. Under these assumptions, the flow model is illustrated with help of following equations[28,31]:

$$\frac{\partial u}{\partial x}+\frac{\partial v}{\partial y}=0, \tag{1}$$

$$u\frac{\partial u}{\partial x}+v\frac{\partial v}{\partial y}+\lambda\left(u^2\frac{\partial^2 u}{\partial x^2}+v^2\frac{\partial^2 u}{\partial y^2}+2uv\frac{\partial^2 u}{\partial x\partial y}\right)=\frac{1}{\rho_f}\frac{\partial}{\partial y}\left(\tilde{\tilde{\mu}}(T)\frac{\partial u}{\partial y}\right)-\frac{\sigma B_o^2}{\rho_f}\left(u+\lambda v\frac{\partial u}{\partial y}\right), \tag{2}$$

$$u\frac{\partial T}{\partial x}+v\frac{\partial T}{\partial y}=\frac{1}{\rho c_p}\frac{\partial}{\partial y}\left(\tilde{\tilde{K}}(T)\frac{\partial T}{\partial y}\right)-\frac{1}{\rho c_p}\frac{\partial q_r}{\partial y}+\frac{Q_0}{\rho c_p}(T-T_\infty)+\tau\left\{D_B\left(\frac{\partial C}{\partial y}\frac{\partial T}{\partial y}\right)+\left(\frac{D_T}{T_\infty}\right)\left(\frac{\partial T}{\partial y}\right)^2\right\}, \tag{3}$$

$$u\frac{\partial C}{\partial x}+v\frac{\partial C}{\partial y}=D_B\frac{\partial^2 C}{\partial y^2}+\left(\frac{D_T}{T_\infty}\right)\frac{\partial^2 T}{\partial y^2}-kr^2(C-C_\infty)\left(\frac{T}{T_\infty^n}\right)\exp\left(-\frac{E_a}{k_1 T}\right). \tag{4}$$

$$u\frac{\partial n}{\partial x}+v\frac{\partial n}{\partial y}+\frac{\hat{b}\hat{w}}{(C_w-C_\infty)}\left[\frac{\partial}{\partial y}\left(n\frac{\partial C}{\partial y}\right)\right]=D_m\frac{\partial^2 n}{\partial y^2}, \tag{5}$$

The appropriate conditions are

$$u=u_w(x)=cx,\ v=0,\ -k\frac{\partial T}{\partial y}=h_1(T_w-T),\ D_B\frac{\partial C}{\partial y}+\frac{D_T}{T_\infty}\frac{\partial T}{\partial y}=0, n=n_w \text{ at } y=0 \tag{6}$$

$$u\to 0, T\to T_\infty,\ C\to C_\infty, n\to n_\infty, \text{when } y\to\infty. \tag{7}$$

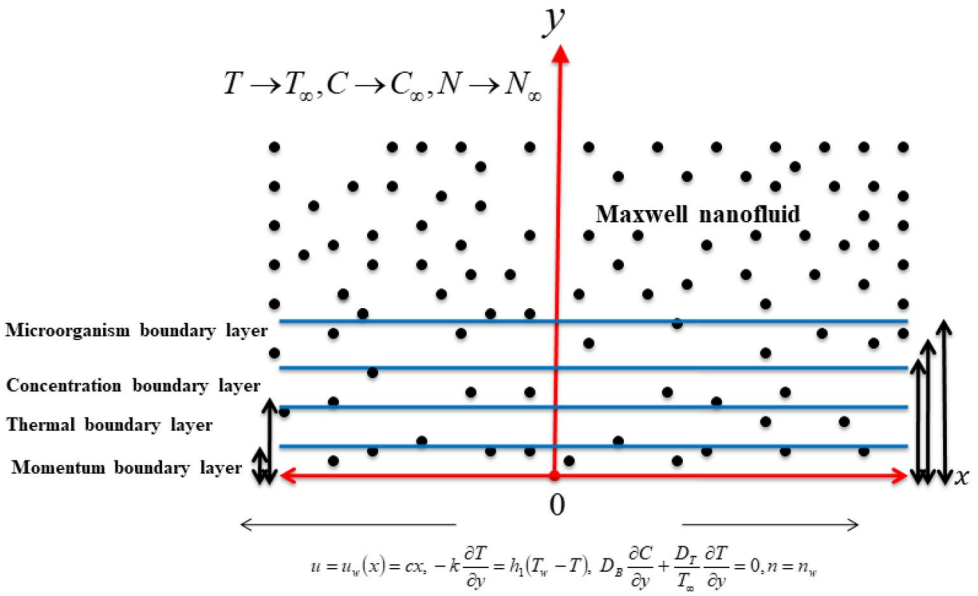

Figure 1. Flow geometry of problem.

with physical quantities like relaxation time λ, fluid density ρ_f, temperature dependent viscosity $\tilde{\tilde{\mu}}(T)$, electrical conductivity σ, magnetic field strength B_0, specific heat ρc_p, variable thermal conductivity $\tilde{\tilde{K}}(T)$, radiative flux q_r, heat source coefficient Q_0, Brownian diffusion D_B, chemotaxis constant $\hat{b}$, mean absorption coefficient k^* and microorganisms diffusion constant D_m.

Defining the radiative flux:

$$\frac{\partial q_r}{\partial y} = -\frac{16\sigma^* T_\infty^3}{3K^*}\frac{\partial^2 T}{\partial y^2}, \tag{8}$$

where σ^* and K^* are Stefan Boltzmann constant and mean absorption coefficient. The expression of viscosity is[18]

$$\tilde{\tilde{\mu}}(T) = \tilde{\tilde{\mu}}_o \exp\left[-a(T - T_\infty)\right]. \tag{9}$$

Now thermal conductivity is:

$$\tilde{\tilde{K}}(T) = K \exp\varepsilon\left(\frac{T - T_\infty}{T_w - T_\infty}\right). \tag{10}$$

Let us define new variables:

$$\eta = \sqrt{\frac{c}{\nu}}y,\ \psi = \sqrt{c\nu}xf(\eta),\ \theta(\eta) = \frac{T - T_\infty}{T_w - T_\infty},\ \varphi(\eta) = \frac{C - C_\infty}{C_w - C_\infty}, \chi(\eta) = \frac{n - n_\infty}{n_w - n_\infty} \tag{11}$$

$$u = \frac{\partial \psi}{\partial y} = cxf'(\eta),\ v = -\frac{\partial \psi}{\partial x} = \sqrt{c\nu}f(\eta).$$

The resulting dimensionless system is:

$$(1 - \gamma_1\theta)\left[f''' - \gamma_1\theta' f''\right] - \beta\left((f)^2 f''' - 2ff'f''\right) - (f')^2 + ff'' = M\left(f' - \beta ff''\right), \tag{12}$$

$$\left(1 + \in \theta + \frac{4}{3}R_d\right)\theta'' = - \in (\theta')^2 - \Pr\left(f\theta' + Q\theta + N_b\theta'\varphi' + N_t(\theta')^2\right), \tag{13}$$

$$\phi'' + Le\Pr f\varphi' + \frac{N_t}{N_b}\theta'' - \Pr Le(1 + \delta\theta)^n \exp\left(\frac{-E}{1 + \delta\theta}\right)\phi = 0, \tag{14}$$

$$\chi'' + Lbf\chi' - Pe\left[\phi''(\chi + \delta_1) + \chi'\phi'\right] = 0, \tag{15}$$

with:

$$\left.\begin{aligned} &f(0) = 0,\ f'(0) = 1,\ f'(\infty) \to 0,\\ &\theta'(0) = -Bi(1 - \theta(0)),\ \theta(\infty) \to 0,\\ &N_b\varphi'(0) + N_t\theta'(0) = 0,\ \varphi(\infty) \to 0.\\ &\chi(0) = 1, \chi'(\infty) \to 0. \end{aligned}\right\} \tag{16}$$

In above mathematical expression, $\Pr$ the Prandtl number, γ_1 the Biot number, R_d the radiation parameter, Le the Lewis number, β the Maxwell parameter, M Hartmann parameter, N_b the Brownian motion parameter, N_t the thermophoresis parameter, ε the curie temperature parameter and Q the heat source/sink parameter, microorganism difference parameter δ_1 Peclet number Pe

$$\Pr = \frac{\mu c_p}{k},\ \gamma_1 = c(T_w - T_\infty),\ Rd = \frac{4\sigma^* T_\infty^3}{3K^*K},\ Le = \frac{\nu}{D_B}, M = \frac{\sigma B_o^2}{\rho_f c},$$
$$\beta = \lambda c,\ N_b = \frac{\tau D_B(C_w - C_\infty)}{\nu}, N_t = \frac{\tau(T_w - T_\infty)}{\nu T_\infty},\ \varepsilon = \frac{T_\infty}{T_w - T_\infty},\ Q = \frac{Q_0}{\rho c_p}.$$

$$\delta_1 = \frac{N_\infty}{N_w - N_\infty},\ Pe = \frac{\hat{b}\hat{w}}{D_m}$$

The dimensionless skin friction coefficient C_{fx}, local Nusselt number Nu_x and the local Sherwood number Sh_x, motile density number Nn_x is:

$$\begin{aligned}
(Re_x)^{1/2}C_{f_x} &= (1-\gamma_1\theta(0))f''(0),\\
(Re_x)^{-1/2}Nu_x &= -\left(1+\frac{4}{3}Rd\right)\theta'(0),\\
(Re_x)^{-1/2}Sh_x &= -\varphi'(0),\\
(Re_x)^{-1/2}Nn_x &= -\chi'(0),
\end{aligned} \tag{17}$$

where $Re_x = U_w(x)x/\nu$ is local Reynolds number.

Computational procedure

The numerical computations are carried out for tracking the solution of desired formulated systems. The shooting technique is implemented to perform the approximate solution. The motivations for utilizing the numerical scheme is due to excellent accuracy. The residual error associated to this scheme is also very convincing. Moreover, this scheme does not involve any complicated discretization steps like other numerical algorithms. For this purpose, the initial value system is obtained. The simulations are carried out under following assumptions:

$$\begin{aligned}
&f = y_1, f' = y_2, f'' = y_3, f''' = y_3', \theta = y_4, \theta' = y_5, \theta'' = y_5',\\
&\phi = y_6, \phi' = y_7, \phi'' = y_7', \chi = y_8, \chi' = y_9, \chi'' = y_9'
\end{aligned} \tag{18}$$

$$y_3' = \left(\frac{1}{1-\gamma_1 y_4-\beta y_1^2}\right)\left[\gamma_1\left(1-\gamma_1 y_4\right)y_3 y_5 + y_2^2 - y_1 y_3 - 2\beta y_1 y_2 y_3 + M y_1 - \beta M y_1 y_3\right] \tag{19}$$

$$y_5' = \left(\frac{-1}{1+\varepsilon y_4-\frac{4}{3}\overset{?}{R}_d}\right)\left[\varepsilon y_5^2 + \Pr\left(y_1 y_5 + Q y_4 + N_b y_5 y_7 + N_t y_5^2\right)\right] \tag{20}$$

$$y_7' = -\Pr Le y_1 y_7 - \frac{N_t}{N_b} y y_2 - \Pr(Le)\left(1+\delta y_4\right)\exp\left(\left(\frac{-E}{1+\delta y_4}\right)y_6\right) \tag{21}$$

$$y_9' = -\left(Lbf y_9 - Pe\left[y_5'\left(y_8+\delta_1\right) + y_9 y_7\right]\right), \tag{22}$$

along with initial conditions

$$\left.\begin{aligned}
&y_1(0) = 0,\ y_2(0) = 1,\ y_2(\infty) \to 0,\\
&y_5(0) = -Bi\left(1-y_5(0)\right),\ y_4(\infty) \to 0,\\
&Nby_7(0) + Nty_4(0) = 0,\ y_7(\infty) \to 0.\\
&y_8(0) = 1, y_8'(\infty) \to 0.
\end{aligned}\right\} \tag{23}$$

Validation of results

The results are validated and verified in Table 1. The comparative analysis is worked out under limiting case with studies of Chen[29] and Iqbal et al.[14]. A fine accuracy of current results is noted with these available investigations.

Results and discussion

Now, the physical aspects of parameters in given flow problem is observed. For this purpose, a graphical analysis is prepared to investigate the thermal phenomenon. In order to analyze the graphical results, the numerical values assigned to parameters are $\Pr = 0.5, \gamma_1 = 0.2, R_d = 0.5, Le = 0.3, \beta = 0.5, M = 0.4, N_b = 0.3,, N_t = 0.3, \varepsilon = 0.2$, $Q = 0.4$, $\delta_1 = 0.2$ and $Pe = 0.5$. Figure 2a preserves observations for velocity f' by utilizing the values of β. A slower velocity impact is observed when β attributed maximum values. Such control in velocity is due to property of relaxation time as fluid takes time to attains its original position. Figure 2b pronouncing the predication in f' upon enriching Hartmann number M. As expected, velocity reduces effectively for M which can be justifies due to role of Lorentz force. Figure 1c predicts that f' increases for enlarging variable viscosity constant γ_1. Figure 3a aims to express the change in temperature θ when β is maximum. The upshot behavior of temperature has been noted for enlarging β. The physical interpretation of variable thermal conductivity constant ε on θ is predicted in

Pr	Chen[29]	Iqbal et al.[14]	Present results
0.72	0.46315	0.46315	0.46315
1.0	0.58199	0.58199	0.58199
3.0	1.16523	1.16523	1.16522
7.0	1.89537	1.89537	1.89538

Table 1. Comparative analysis for $-\theta'(0)$ with Chen[26] and Iqbal et al.[14].

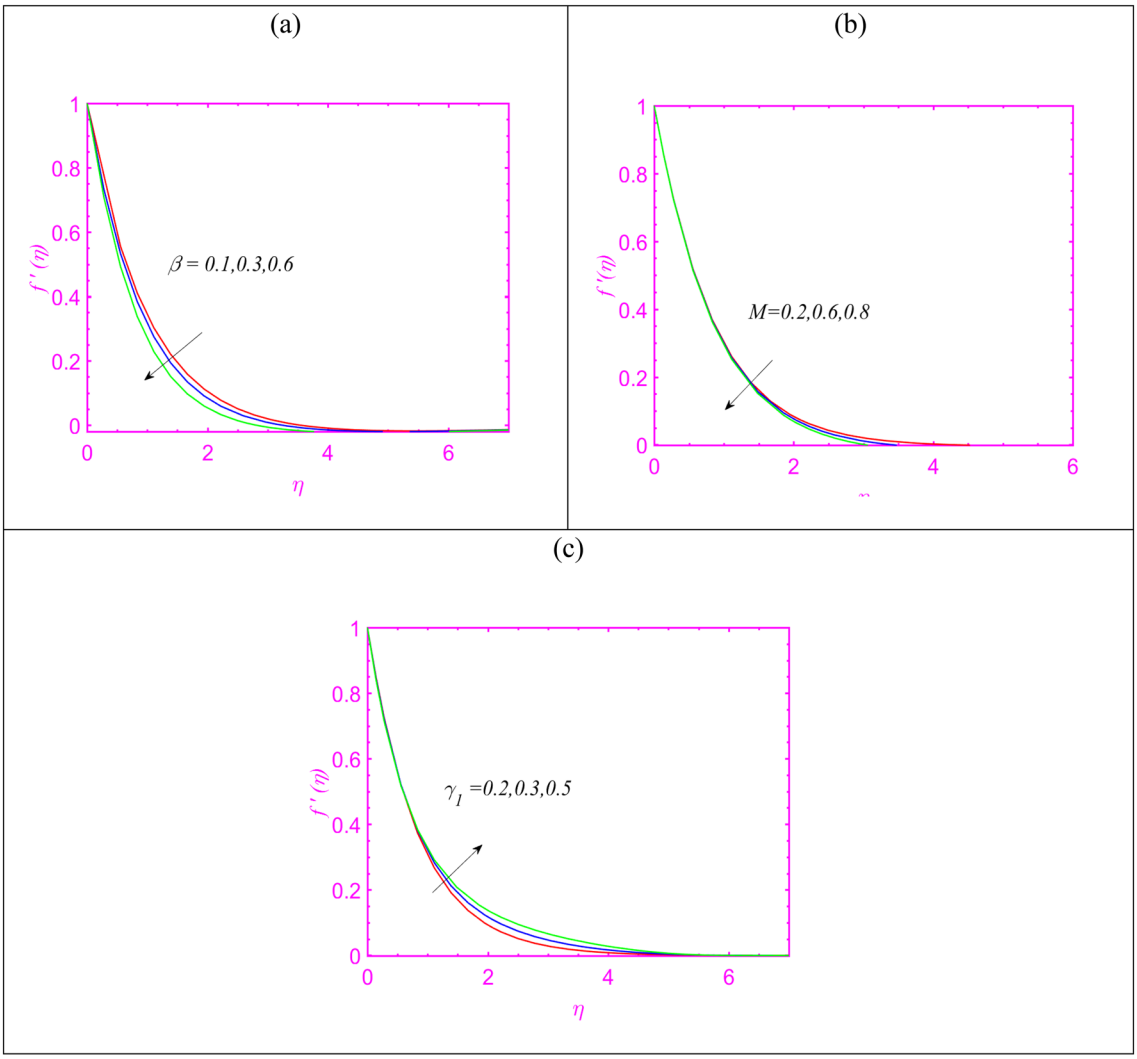

Figure 2. (**a**–**c**) Change in velocity for (**a**) β, (**b**) M and (**c**) γ_1.

Fig. 3b. The thermal profile gets more maximum trend subject to increase ε. In fact, the consideration of variable thermal conductivity fluctuated the heat transfer phenomenon more effectively as it varies with various factors. Figure 3c imposed the role of radiation constant Rd on θ. The presence of radiative phenomenon incorporated more heat transfer impact and boosted the thermal pattern. The radiative phenomenon is associated to the transmission of energy in terms of electromagnetic waves. Figure 3d discusses the onset of Prandtl number Pr on θ. The reduction is noted for temperature due to enlarging Pr. Physically, such effects are due to controls of thermal diffusivity which preserving opposite relation with Prandtl number.

In order to evaluate the characteristics of heat source Q on θ, Fig. 4a has been presented. Physically, the presence of Q identifying some external heat source which can increases the heat transfer determination. In order to discuss the contribution of Nb and Nt on θ, Fig. 4b,c are plotted, respectively. First, increasing outcomes in heat transfer fluctuation are noted due to both Nb and Nt. The increasing in heating capacitance due to Nb is justified as nanoparticles specifies random motion due to which increment in θ is noted. On other hand, the thermophoresis parameter justifies the migration of fluid in relatively cooler regime which results in increment in temperature. The effects of Biot number Bi on θ is examined in Fig. 4d. The enhancing change is noticed for θ with increasing Bi. Physically, the Biot number is associated to the heat transfer coefficient which enriches the heat transfer impact.

Figure 5a presents the concentration profile ϕ in view of leading aspects of activation energy constant E. The concentration profile enriches when the effects of activation energy are utilized. The activation energy is

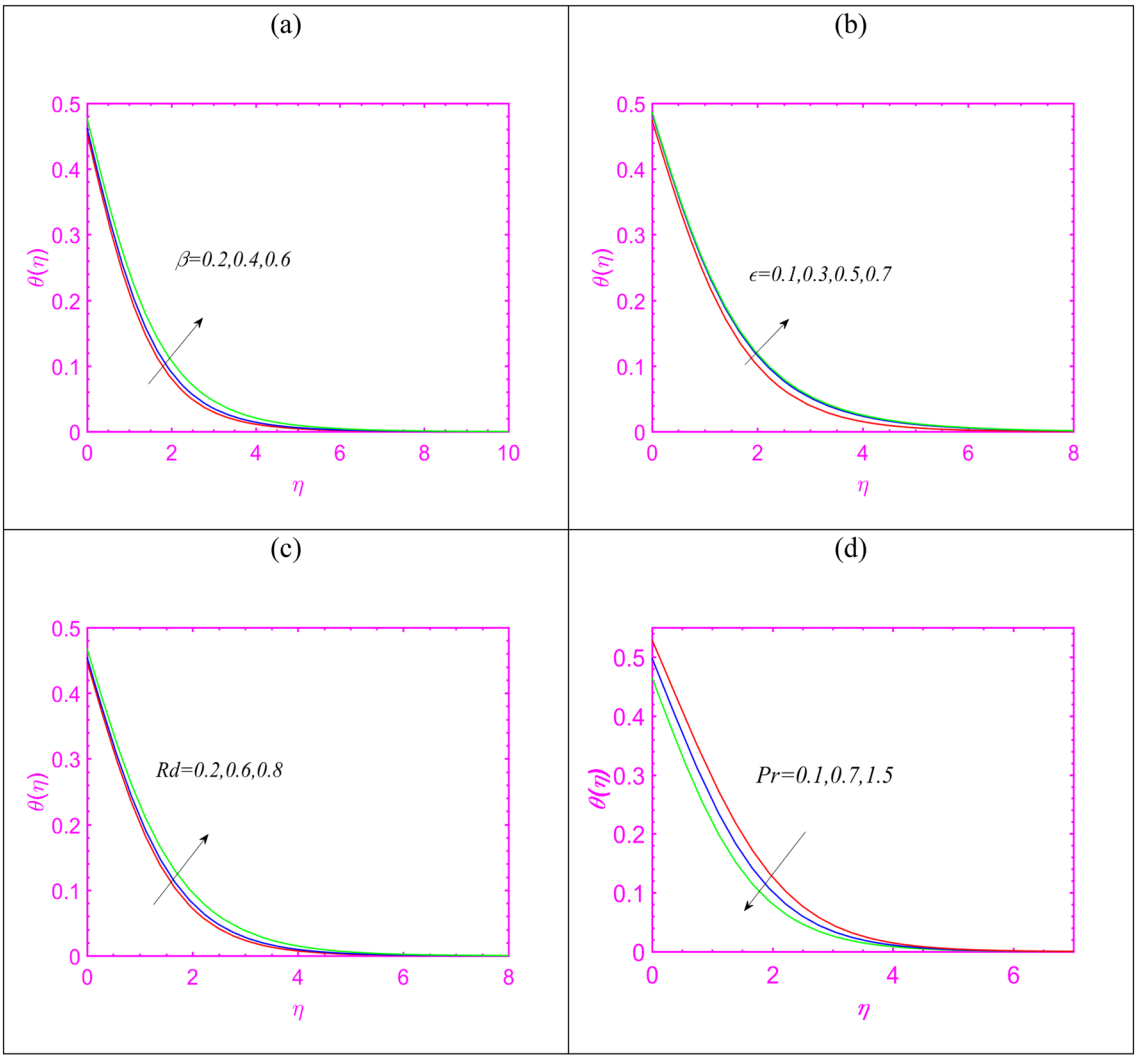

Figure 3. (**a**–**d**) Assessment of temperature for (**a**) β, (**b**) ε, (**c**) Rd and (**d**) Pr .

important in initiating the chemical reaction process. Figure 5b justifying the importance of Brownian constant Nb on ϕ. Here, the declining rate of concentration is exhibited for Nb. Figure 5c demonstrates that ϕ reduces with γ_1. The graphical effectors made in Fig. 5d reporting the insight of ϕ due to enriching values of Lewis number Le. The Lewis number expresses contrasting relation with mass diffusivity which turning down concentration phenomenon. Figure 6a is presented in order to judge the influence of Peclet number Pe on microorganisms profile χ. Lower observations are scaled out for χ in view of increasing Pe. Physical aspects behind such change is smaller motile density. Same results are examined in Fig. 6b in case of increasing Lb. Figure 6c claims that χ boosted for increasing M.

Table 2 identifies the numerical calculation of wall shear force under the variation of emerging parameters. Larger variation in $-f''(0)$ is observed for β. However, decreasing aspect of $-f''(0)$ is reported for γ_1. Table 3 presents change in $-\theta'(0)$ due to different constants. It is noted that $-\theta'(0)$ declined for ε, Q and Nb. From Table 4, it is examined that $-\phi'(0)$ gets maximum variation for Le while less results are predicted for β. Table 5 claims an increasing results for $-\chi'(0)$ against Pe and Lb.

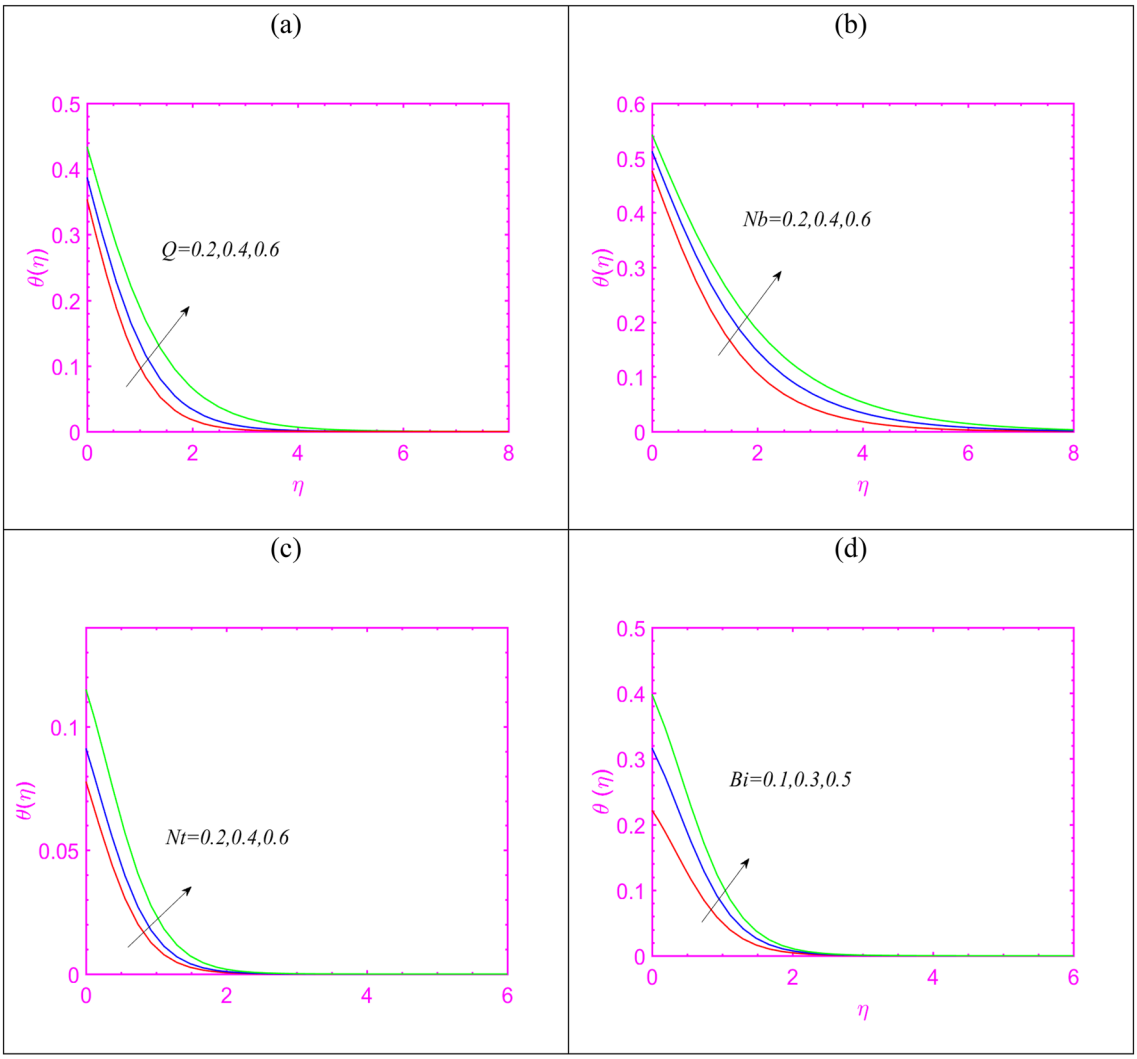

Figure 4. (**a**–**d**) Assessment of temperature for (**a**) *Q*, (**b**) *Nb*, (**c**) *Nt* and (**d**) *Bi*.

Conclusions

The bioconvective flow of Maxwell nanofluid under the assumptions of variable thermal conductivity and slip effects have been studied. The novel contribution of radiative phenomenon and activation energy is endorsed. The shooting technique is utilized for solving to problem. Major results are:

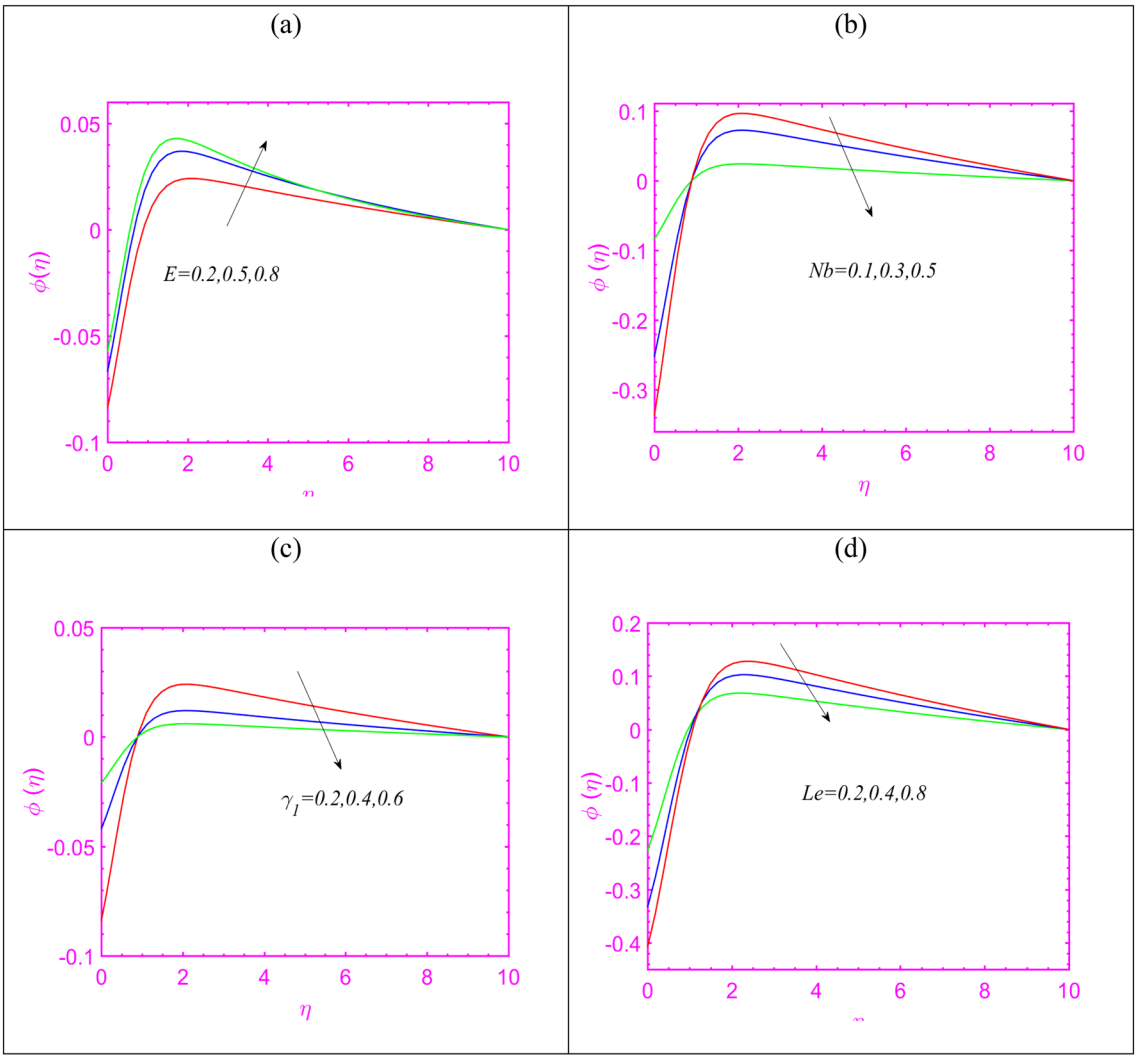

Figure 5. (**a**–**d**) Assessment of temperature for (**a**) E, (**b**) Nb, (**c**) γ_1 (**d**) Le.

- A reduction in velocity profile is noticed due to relaxation time constant.
- An increment in velocity is exhibited due to variable viscosity constant.
- The variable thermal conductivity parameter enhanced the temperature profile more effectively s compared to constant assumptions of thermal conductivity.
- The temperature profile enhanced due to relaxation constant.

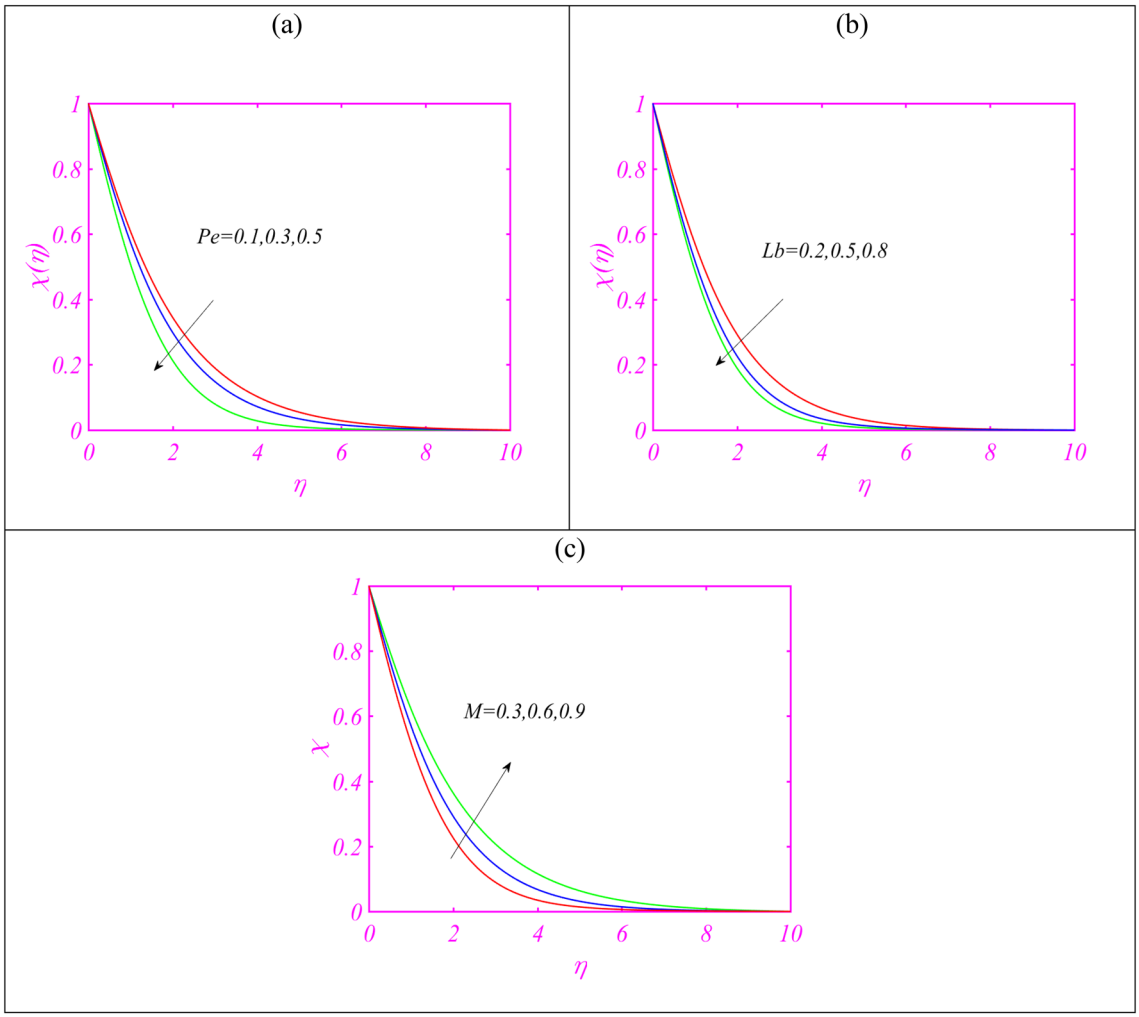

Figure 6. (**a**–**c**) Assessment of microorganism profile for (**a**) *Pe*, (**b**) *Lb* (**c**) *M*.

M	β	γ_1	$-f''(0)$
0.2	0.1	0.1	0.589053
0.4			0.645329
0.6			0.690325
	0.4		0.7874201
	0.8		0.842655
	1.2		0.8948755
		0.1	0.924547
		0.3	0.914624
		0.5	0.854766

Table 2. Numerical calculation of $-f''(0)$.

- By increasing Biot number and external heat source, the heat transfer phenomenon boosted.
- The microorganisms profile enhanced with Hartmann constant.
- These results can be further updated by utilizing the cubic autocatalysis chemical reaction, thermos-diffusion effects and Joule heating[30,31].

ε	Rd	Pr	Q	Nb	$-\theta'(0)$
0.1					0.352164
0.3					0.284876
0.5					0.2446830
	0.2				0.365648
	0.4				0.454648
	0.6				0.581325
		0.3			0.458895
		0.7			0.614654
		0.9			0.98322
			0.2		0.484565
			0.4		0.436889
			0.8		0.41598
				0.2	0.513265
				0.4	0.487798
				0.7	0.435488

Table 3. Numerical calculation of Nusselt number.

β	Nt	Le	$-\varphi'(0)$
0.2	0.1	0.3	0.3165658
0.4			0.2548766
0.6			0.184565
0.1	0.1		0.3579889
	0.3		0.3423215
	0.5		0.297988
		0.2	0.3598988
		0.6	0.4523565
		0.8	0.4987820

Table 4. Numerical calculation of Sherwood number.

Pe	Lb	$-\chi'(0)$
0.1	0.5	0.5145465
0.3		0.5698899
0.7		0.6245565
0.2	0.2	0.5045666
	0.4	0.5854798
	0.6	0.648778

Table 5. Numerical calculation of motile density number.

Data availability

The datasets used and/or analyzed during the current study available from the corresponding author on reasonable request.

Received: 16 September 2023; Accepted: 30 December 2023
Published online: 17 January 2024

References

1. Choi, S. U. S. Enhancing thermal conductivity of fluids with nanoparticles. *ASME Pub Fed.* **231**, 99–106 (1995).
2. Kumar, K. G. Exploration of flow and heat transfer of non-Newtonian nanofluid over a stretching sheet by considering slip factor. *Int. J. Numer. Method H* **30**(4), 1991–2001 (2019).
3. Santos, T. F., Santos, C. M., Aquino, M. S., Oliveira, F. R. & Medeiros, J. I. Statistical study of performance properties to impact of Kevlar® woven impregnated with Non-Newtonian Fluid (NNF). *J. Mater. Res. Technol.* **9**(3), 3330–3339 (2020).

4. Sohail, M. & Naz, R. Modified heat and mass transmission models in the magnetohydrodynamic flow of Sutterby nanofluid in stretching cylinder. *Phys. A* **549**, 124088 (2020).
5. Muhammad, K., Hayat, T., Alsaedi, A. & Ahmad, B. Melting heat transfer in squeezing flow of basefluid (water), nanofluid (CNTs+ water) and hybrid nanofluid (CNTs+ CuO+ water). *J. Therm. Anal. Calorimetry* **143**, 1157–1174 (2021).
6. Babazadeh, H., Zeeshan, A., Jacob, K., Hajizadeh, A. & Bhatti, M. M. Numerical modelling for nanoparticle thermal migration with effects of shape of particles and magnetic field inside a porous enclosure. *Iran J. Sci. Technol. Trans. Mech. Eng.* https://doi.org/10.1007/s40997-020-00354-9 (2020).
7. Alqarni, M. S., Yasmin, S., Waqas, H. & Khan, S. A. Recent progress in melting heat phenomenon for bioconvection transport of nanofluid through a lubricated surface with swimming microorganisms. *Sci. Rep.* **12**(1), 8447 (2022).
8. Saeed, A. *et al.* Darcy-Forchheimer MHD hybrid nanofluid Flo8w and heat transfer analysis over a porous stretching cylinder. *Coatings* **10**(4), 391 (2020).
9. Hamrelaine, S. *et al.* Analytical investigation of hydromagnetic ferro-nanofluid flowing via rotating convergent/divergent channels. *Eur. Phys. J. Plus.* **137**, 1291 (2022).
10. Shahzad, F. *et al.* The effect of pressure gradient on MHD flow of a tri-hybrid Newtonian nanofluid in a circular channel. *J. Magn. Magn. Mater.* **568**, 170320 (2023).
11. Acharya, S. Effect of cavity undulations and thermal boundary conditions on natural convection and entropy generation in CuO-water/Al2O3-water nanofluid. *J. Nanofluids* **12**(3), 687–698 (2023).
12. Sajid, T. *et al.* Quadratic regression analysis for nonlinear heat source/sink and mathematical Fourier heat law influences on Reiner-Philippoff hybrid nanofluid flow applying Galerkin finite element method. *J. Magn. Magn. Mater.* **568**, 170383 (2023).
13. Hanif, H. *et al.* Numerical Crank-Nicolson methodology analysis for hybridity aluminium alloy nanofluid flowing based-water via stretchable horizontal plate with thermal resistive effect. *Case Stud. Therm. Eng.* **42**, 102707 (2023).
14. Iqbal, Z., Mehmood, R., Ahmad, B. & Maraj, E. N. Combined impact of viscosity variation and Lorentz force on slip flow of radiative nanofluid towards a vertical stretching surface with convective heat and mass transfer. *Alex. Eng. J.* **57**, 3189–3197 (2018).
15. Mabood, F. Numerical simulations for swimming of gyrotactic microorganisms with Williamson nanofluid featuring Wu's slip, activation energy and variable thermal conductivity. *Appl. Nanosci.* **13**, 131–144 (2023).
16. Chu, Y.-M. *et al.* Mathematical modeling and computational outcomes for the thermal oblique stagnation point investigation for non-uniform heat source and nonlinear chemical reactive flow of Maxwell nanofluid. *Case Stud. Thermal Eng.* **41**, 102626 (2023).
17. Alwatban, A. M., Khan, S. U., Waqas, H. & Tlili, I. Interaction of Wu's slip features in bioconvection of Eyring Powell nanoparticles with activation energy. *Processes* **7**(11), 859 (2019).
18. Khan, M. I., Haq, F., Khan, S. A., Hayat, T. & Imran Khan, M. Development of thixotropic nanomaterial in fluid flow with gyrotactic microorganisms, activation energy, mixed convection. *Comput. Methods Prog. Biomed.* **187**, 105186 (2020).
19. Khan, N. S. *et al.* Entropy generation in bioconvection nanofluid flow between two stretchable rotating disks. *Sci. Rep.* **10**, 4448 (2020).
20. Bafakeeh, O. T. *et al.* On the bioconvective aspect of viscoelastic micropolar nanofluid referring to variable thermal conductivity and thermo-diffusion characteristics. *Bioengineering* **10**(1), 73 (2023).
21. Khan, M. I. *et al.* Slip flow of micropolar nanofluid over a porous rotating disk with motile microorganisms, nonlinear thermal radiation and activation energy. *Int. Commun. Heat Mass Transfer* **122**, 105161 (2021).
22. Bhatti, M. M., Al-Khaled, K., Khan, S. U., Chammam, W. & Awais, M. Darcy-Forchheimer higher order slip flow of Eyring-Powell nanofluid with nonlinear thermal radiation and bioconvection phenomenon. *J. Disp. Sci. Technol.* **44**(2), 225–235 (2023).
23. Irfan, M. Energy transport phenomenon via Joule heating and aspects of Arrhenius activation energy in Maxwell nanofluid. *Waves Random Complex Media* **1**, 1–16 (2023).
24. Ali, U., Irfan, M., Akbar, N. S., Ur Rehman, K. & Shatanawi, W. Dynamics of Soret-Dufour effects and thermal aspects of Joule heating in multiple slips Casson-Williamson nanofluid. *Int. J. Mod. Phys. B* **24**, 50206 (2023).
25. Irfan, M. Study of Brownian motion and thermophoretic diffusion on non-linear mixed convection flow of Carreau nanofluid subject to variable properties. *Surf. Interfaces* **23**, 100926 (2021).
26. Ahmad, M. *et al.* Forced convection three-dimensional Maxwell nanofluid flow due to bidirectional movement of sheet with zero mass flux. *Int. Commun. Heat Mass Transfer* **135**, 106050 (2022).
27. Ahmad, B. *et al.* Thermal diffusion of Maxwell nanoparticles with diverse flow features: Lie Group simulations. *Int. Commun. Heat Mass Transfer* **136**, 106164 (2022).
28. Saeed, M. *et al.* Heat and mass transfer inspection for slip flow of radiative Maxwell fluid when role of thermal conductivity and viscosity is variable: A Reynolds viscosity model. *J. Indian Chem. Soc.* **99**(10), 100709 (2022).
29. Chen, C. H. Laminar mixed convection adjacent to vertical continuously stretching sheet. *Heat Mass Transfer* **33**, 471–476 (1998).
30. Irfan, M. *et al.* Significance of non-Fourier heat flux on ferromagnetic Powell-Eyring fluid subject to cubic autocatalysis kind of chemical reaction. *Int. Commun. Heat Mass Transfer* **138**, 106374 (2022).
31. Irfan, M. Influence of thermophoretic diffusion of nanoparticles with Joule heating in flow of Maxwell nanofluid. *Num. Methods Part. Diff. Equ.* **39**(2), 1030–1041 (2023).

Acknowledgements

The author extends the appreciation to the Deanship of Postgraduate Studies and Scientific Research at Majmaah University for funding this research work through the project number R-2024-919.

Author contributions

H.H. and I.T. wrote the main manuscript text perform conceptualization, data curation, formal analysis, methodology, and revised version.

Competing interests

The authors declare no competing interests.

Additional information

Correspondence and requests for materials should be addressed to I.T.

Reprints and permissions information is available at www.nature.com/reprints.

Publisher's note Springer Nature remains neutral with regard to jurisdictional claims in published maps and institutional affiliations.

Open Access This article is licensed under a Creative Commons Attribution 4.0 International License, which permits use, sharing, adaptation, distribution and reproduction in any medium or format, as long as you give appropriate credit to the original author(s) and the source, provide a link to the Creative Commons licence, and indicate if changes were made. The images or other third party material in this article are included in the article's Creative Commons licence, unless indicated otherwise in a credit line to the material. If material is not included in the article's Creative Commons licence and your intended use is not permitted by statutory regulation or exceeds the permitted use, you will need to obtain permission directly from the copyright holder. To view a copy of this licence, visit http://creativecommons.org/licenses/by/4.0/.

© The Author(s) 2024